Simulation of the Majorana equation in circuit QED

Sheng Liu,[1] Chuan-Jia Shan,[1] Zhi-Ming Zhang,[2] and Zheng-Yuan Xue*[1]

[1]*Laboratory of Quantum Information Technology, and School of Physics and Telecommunication Engineering, South China Normal University, Guangzhou 510006, China*

[2]*Laboratory of Photonic Information Technology, LQIT, and SIPSE, South China Normal University, Guangzhou 510006, China*

(Dated: April 3, 2013)

We propose a scheme to simulate the 1D Majorana equation with two Cooper pair boxes coupled to a 1D superconducting transmission line resonator, where strong coupling limit can be achieved. With proper chosen of systematic parameters, we are able to engineer different kinds of interaction, which is indispensable in simulating the Majorana equation in an enlarged real Hilbert space. Measurement of the conserved observable of pseudo-helicity via transmission spectrum of the cavity field can verify the simulated Majorana wave function. The measurement results are experimentally resolvable based on our estimation with conservative parameters.

PACS numbers: 03.67.Lx, 42.50.Dv, 74.78.Na

Keywords: Quantum computation, Majorana-fermion, Aharonov-Casher effect, parity measurements

The request for a quantum simulator is because that it allows for the study of quantum systems that beyond the reach of classical computers. Meanwhile, it is expected to be more robust against virous imperfections than a quantum computer [1]. One of the successful cases is the quantum simulation of the Dirac equation, which combines quantum mechanics and special relativity [2]. In certain regime, electrons in graphene may behavior as Dirac fermions, which has recently raised strong interest in condensed-matter physics [3]. Meanwhile, it is proposed that ultracold atoms in an optical lattice can be used to simulate relativistic Dirac fermions [4]. Compared with graphene, the atomic simulation may offer more controllability. Alternatively, simulation of the Dirac equation is also proposed in cold atoms [5] with light-induced gauge potential [6, 7]. Meanwhile, quantum simulation of the Dirac equation in trapped ions system is also proposed [8] and been experimentally confirmed [9].

One of the greatest success of the Dirac equation is that it predicts the existence of antiparticle of electron. In viewing of the success of the Dirac Equation, Majorana inquired whether it is possible that a particle to be its own antiparticle. As a result, he found an equation that such particle would satisfy, i.e., the Majo-

* xuezhengyuan@yahoo.com.cn

rana equation (ME) [10]. Recently, it is proposed that ME can be simulated with trapped ions [11], which is developed in an enlarged Hilbert space: an 1D Majorana equation is transformed to a 3D Dirac equation with dimensional reduction, i.e., momenta in y and z directions are zero. The simulation of the ME is not straightforwardly as it is non-Hermitian, i.e., one needs to implement the complex conjugation of Majorana wave function. Therefore, it needs new toolbox to access the unphysical operations in the simulation.

Superconducting system is generally regarded as one of the most promising candidates for physical implementation of qubit that can support scalable quantum information processing [12, 13]. Recently, quantum simulators using superconducting quantum circuits have attracted much attention [14]. With mature microchip fabrication techniques, it can be used to simulate quantum system in a flexible way. Here, we consider the simulation of ME with two Cooper pair boxes (CPB) capacitively coupled to an 1D transmission line resonator (TLR) [15], where elements are mesoscopic circuit excitations. Therefore, it provides an interesting example of simulating physics associated with relativistic ME in a mesoscopic circuit. As the simulation in Ref. [11] is based on complex-to-real map, which transforms a Majorana equation into a higher dimensional Dirac equation, for 2D or 3D ME simulation, one needs more qubit (more than 3) to simulate the transformed Hamiltonian. Unfortunately, in trapped-ion systems, the individual addressing is difficult for large arrays ($N > 3$) [16]. Comparing with the trapped ion simulation, a distinct feature of the present proposal is that the combination of individual addressing with a many CPB setup is feasible.

A ME reads

$$i\hbar\gamma^{\mu}\partial_{\mu}\psi = mc\psi_c, \tag{1}$$

where c is the speed of light, m is mass, γ^{μ} with μ=1, 2, 3, and 4 are the Dirac matrices, and $\psi_c = i\gamma^2\mathcal{K}\psi$ is a charge conjugation field with $\mathcal{K}$ being a complex conjugation operator. For 1D case, $\psi_c = \mathcal{C}\sigma_z\psi^*$, where $\mathcal{C}$ is a unitary matrix satisfying $\mathcal{C}\gamma^T = -\gamma\mathcal{C}$ with $\gamma = i\sigma_x\sigma_z$. Then we can choose $\mathcal{C} = i\sigma_y$ in a suitable basis, i.e., $\psi_c = i\sigma_y\sigma_z\mathcal{K}\psi = i\sigma_y\sigma_z\psi^*$. Then, ME in 1D reads

$$i\hbar\partial_t\psi = (c\sigma_x p_x - imc^2\sigma_y\mathcal{K})\psi. \tag{2}$$

where ψ is a two-component complex spinor, $p_x = -i\hbar\partial_x$ is the momentum operator in x direction.

To make the nonphysical complex conjugation $\psi \to \mathcal{K}\psi = \psi^*$ implementable, one may map the two-component complex spinor into a four-component real spinor [11], that is,

$$\psi = \begin{pmatrix} \psi_1 \\ \psi_2 \end{pmatrix} \in \mathbb{C}_2 \to \Psi = \frac{1}{2}\begin{pmatrix} \psi + \psi^* \\ i(\psi^* - \psi) \end{pmatrix} \in \mathbb{R}_4. \tag{3}$$

After this mapping, one can unify all the antiunitary or unitary operators and complex field ψ in an enlarged

Hilbert space. Then, in the enlarged real Hilbert space, Eq. (2) reads

$$i\hbar\partial_t\Psi = [c(\mathbb{E}\otimes\sigma_x)p_x - mc^2\sigma_x\otimes\sigma_y]\Psi, \tag{4}$$

where $\Psi = \begin{pmatrix}\psi_1^r & \psi_2^r & \psi_1^i & \psi_2^i\end{pmatrix}^T \in \mathbb{R}_4$ and it now become an implementable Hamiltonian equation. In Eq. (4), the four components of the spinor is nonlinearly coupled and can not be separated, so it is a $1+1$ Dimension Dirac equation with an irreducible 4 Dimensional Hilbert space notation. In the following, we will simulate the dynamics of ME in 1+1 Dimension by engineering this Hamiltonian. Meanwhile, it is well known that Majorana equation in 3D conserves the observable of helicity. In 1D, helicity reduces to so-called pseudo-helicity $\Sigma = \sigma_x p_x$, and it is still conserved in 1D ME but not in 1D Dirac equation $i\hbar\partial_t\Psi_D = H_D\Psi_D$ with $H_D = c\sigma_x p_x + mc^2\sigma_z$ as $[\Sigma, H_D] \neq 0$. Therefore, measurement of the pseudo-helicity can illustrate the Majorana wave function, and thus to verify our dynamical simulation. Mapping into the real Hilbert space, the pseudo-helicity Σ reads

$$\tilde{\Sigma} = M^\dagger\sigma_x p_x M = (\mathbb{E}\otimes\sigma_x - \sigma_y\otimes\sigma_x)p_x \tag{5}$$

where $\mathbb{E}$ is identity matrix.

We now turn to our circuit QED simulation. The qubit considered here is the superconducting Coopper pair box (CPB) consisting of superconducting island where two Josephson junctions with capacitance C_J and Josephson energy E_j are configured into a loop geometry, which is pierced by an applied external magnetic flux Φ. On condition that Josephson energy is much small than charging energy $E_c = e^2/2C_\Sigma$ ($C_\Sigma = C_g + 2C_J$), restricting the induced charge $N_g = C_g V_g^{dc}/(2e)$ to the range of $N_g \in [0,1]$, only a pair of adjacent charge state on the inland are relevant. Then, the CPB is a simple two-level system described by [13]

$$H_a = -\frac{E_{el}}{2}\bar{\sigma}_z - \frac{E_J}{2}\bar{\sigma}_x, \tag{6}$$

where $\bar{\sigma}_x$, $\bar{\sigma}_z$ are the pauli matrices in the basis of $\{|0\rangle, |1\rangle\}$, $E_{el} = 4E_c(1-2N_g)$ is the electrostatic energy and $E_J = 2E_j\cos(\pi\Phi/\Phi_0)$ is the effective Josephson energy with Φ_0 being the flux quanta. From Eq. (6), one can see that it is possible and convenient to control the qubit by the applied gate voltage V_g^{dc} and the pierced flux Φ [13]. Therefore, the qubit splitting energy can be tunable by the external magnetic flux even with fix gate voltage, e.g., at the degeneracy point $N_g = 1/2$.

In circuit QED, the CPB is capacitively coupled to the center conductor via a capacitance C_g, at the cavity mode's antinode with a maximum voltage. Then, besides the dc control voltage V_g^{dc}, the gate voltage on the CPB also include an ac part from the oscillation of the cavity mode. Taking both parts into consideration lead Eq. (6) to

$$H_{int} = -2E_c\left(1-2N_g^{dc}\right)\bar{\sigma}_z - \frac{E_J}{2}\bar{\sigma}_x + \hbar w_r a^\dagger a - \hbar g\left(a+a^\dagger\right)\left(1-2N_g^{dc}-\bar{\sigma}_z\right), \tag{7}$$

where $a^\dagger$ and a is the creation and annihilation operator of the cavity mode and w_r is its frequency, g is the coupling strength with $g/2\pi \in [5.8, 100]$ MHz [17]. Then, denoting that $\{|\downarrow\rangle, |\uparrow\rangle\}$ are the ground state and the excited state of the first two terms of Hamiltonian (7), respectively. In this new basis, at the degeneracy point, within the rotating-wave approximation, Hamiltonian (7) reduces to the Jaynes-Cummings model [17]

$$H_{JC} = \hbar w_r a^\dagger a + \frac{\hbar\omega}{2}\sigma_z + \hbar g(a^\dagger\sigma_- + a\sigma_+) \tag{8}$$

where $\omega = E_J/\hbar$ and σ_z is pauli matrices in the new basis.

In a circuit QED system, a microwave drive of frequency w_d can be capacitively coupled to the resonator, which can be in the form of

$$H_d(t) = \hbar\varepsilon(t)\left[a^\dagger e^{-i(w_d t-\phi)} + a e^{i(w_d t-\phi)}\right], \tag{9}$$

where $\varepsilon(t)$ and ϕ is the amplitude and the initial phase of the microwave pulse, respectively. All of the local operation on the qubit are rely on w_d, $\varepsilon(t)$ and phase ϕ, which have been experimentally achieved [15]. For the large drive amplitude compare to the vacuum fluctuation of the resonator, the microwave pulse can be treated as a classical field. Make a unitary transformation $U = \exp(\alpha a^\dagger - \alpha^* a)$ on the total Hamiltonian consists of (8) and (9) leads to [18]

$$H_{DJC1} = \hbar w_r a^\dagger a + \frac{\hbar\omega}{2}\sigma_z + \hbar g\left[(a^\dagger + \alpha^*)\sigma_- + H.c.\right]. \tag{10}$$

On condition that the drive amplitude are independent of time, $-\alpha\Delta = \varepsilon\exp[-i(w_d t - \phi)]$ with $\Delta = \omega_r - \omega_d$. In the rotating frame at frequency w_d, we can rewrite (10) as

$$H_{DJC2} = \hbar\Delta a^\dagger a + \hbar g(a^\dagger\sigma_- + a\sigma_+) + \frac{\hbar\delta'}{2}\sigma_z + \frac{\hbar\Omega_d}{2}(\sigma_- e^{-i\phi} + \sigma_+ e^{i\phi}), \tag{11}$$

where $\Omega_d = 2g\varepsilon/\Delta$ and $\delta' = \omega - \omega_d$.

Working in the eigenbasis of the last two terms of the above Hamiltonian, the Hamiltonian (11) becomes

$$H_{DJC3} = \hbar\Delta a^\dagger a + \frac{\hbar\Omega}{2}\sigma_z + \frac{\hbar g}{2}[a e^{-i\phi}(\cos(\theta')\sigma_z - \sin(\theta')\sigma_x + \sigma_+ - \sigma_-) + H.c.], \tag{12}$$

where $\theta' = \arctan(\delta'/\Omega_d)$ and $\Omega = \sqrt{\Omega_d^2 + \delta'^2}$. In the interaction picture, the interaction Hamiltonian of (12) reads [18, 19]

$$H_I = \frac{\hbar g}{2}[a e^{-i\Delta t} e^{-i\phi}(\sigma_z + \sigma_+ e^{i\Omega t} - \sigma_- e^{-i\Omega t}) + \text{H.c.}], \tag{13}$$

which is key to achieve our effective Hamiltonian for simulating ME and we have $\delta' = 2n\pi\Omega_d$ with n being an integer. From this microwave driven Hamiltonian, one can engineer different type of interactions. For

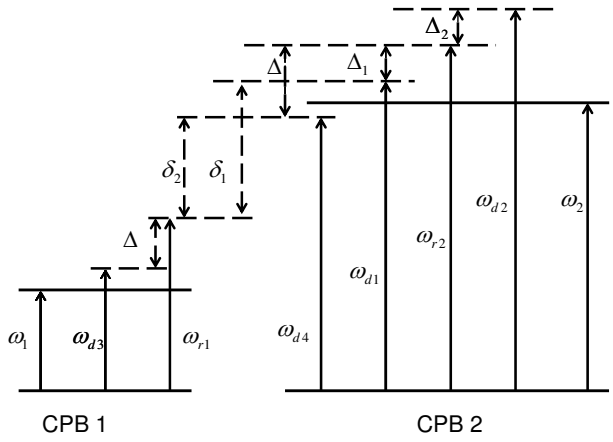

FIG. 1: Level structure of our scheme. ω_1, ω_2 are level separation of the two CPBs, the frequency of the four microwave pulses are ω_{d1}, ω_{d2}, ω_{d3} and ω_{d4}, and ω_{r1} and ω_{r2} are the frequency of the cavity modes.

$\Delta = \Omega$, one obtains

$$H_I' = \frac{\hbar g}{2} a e^{-i\phi}(\sigma_+ + \sigma_z e^{-i\Omega t} - \sigma_- e^{-2i\Omega t}) + \text{H.c.}. \tag{14}$$

In rotating-wave approximation, one can neglect the fast oscillating terms, then the above Hamiltonian reduces to

$$H_1 = \frac{\hbar g}{2}(a\sigma_+ e^{-i\phi} + a^\dagger \sigma_- e^{i\phi}) \tag{15}$$

Similarly, for $\Delta = -\Omega$, one obtains

$$H_2 = -\frac{\hbar g}{2}(a\sigma_- e^{-i\phi} + a^\dagger \sigma_+ e^{i\phi}) \tag{16}$$

Meanwhile, for strong driven $\Omega \gg \Delta$ one obtains

$$H_3 = \frac{\hbar g}{2}(a e^{-i(\Delta t+\phi)} + a^\dagger e^{i(\Delta t+\phi)})\sigma_z. \tag{17}$$

To simulate 1D ME in circuit QED, we use two CPBs with level separation ω_1 and ω_2, four microwave pulses of frequency ω_{d1}, ω_{d2}, ω_{d3} and ω_{d4} with initial phase ϕ_1, ϕ_2, ϕ_3 and ϕ_4, and two cavity modes of frequency ω_{r1} and ω_{r2}. The level structure and the frequency of the driven fields are shown in Fig. 1. As explicitly shown in Eq. (4), there are two components: the first one is the kinetic term of CPB 2 $cp_x(\mathbb{E}\otimes\sigma_x)$ and the second one is the exchange coupling of the two CPBs. As the kinetic term is the combination of Hamiltonian (15) and (16), it can be generated by two detuned driving microwave pulses of frequencies ω_{d1} and ω_{d2} with detuning $\Delta_1 = \omega_{r2} - \omega_{d1} = \Omega_1$ and $\Delta_2 = \omega_{r2} - \omega_{d2} = -\Omega_2$, and the initial phases

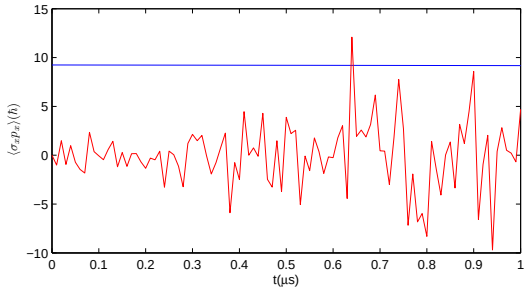

FIG. 2: (color online) Expectation values of pseudohelicity $\Sigma = \sigma_x p_x$ in Dirac equation(red line) and Majorana equation(blue line).

$\phi_1 = \pi/2$ and $\phi_2 = -\pi/2$. In typical experiments, we can choose $\omega_{r2} = 10$ GHz, $\omega_{d1} = 9.9$ GHz and $\omega_{d2} = 10.1$ GHz, thus it is readily to get $\Omega_1 = \Omega_2 = 100$ MHz. Then, we get the combined kinetic term Hamiltonian $i\hbar g(a^\dagger - a)(\mathbb{E} \otimes \sigma_x)/2$ for CPB 2 with level separation of $\omega_2 = 9.7$ GHz. Meanwhile, we on purposely chosen two CPBs with much different splitting energy with $\omega_1 = 4.4$ GHz, and thus ω_{d1} and ω_{d2} can not generate similar kinetic term on CPB 1 on the condition that $\delta_1 = \omega_{d1} - \omega_{r1} = 4.9$ GHz with $\omega_{r1} = 5$ GHz, which is much larger than $\{\Delta_1, |\Delta_2|\} = 100$ MHz. The second term is generated by virtual excitation of the TLR, where we need same detuning between the driving microwave field and the two CPB. As we choose the different CPB splitting energy, we also need two additional strong driving microwave field: $\{\Omega_3, \Omega_4\} \gg \Delta = \omega_{r1} - \omega_{d3} = \omega_{r2} - \omega_{d4} = 500$ MHz. Using effective Hamiltonian (17), with initial phase $\phi_3 = \phi_4 = 0$, we obtain, $\frac{\hbar g}{2}(\sigma_z \otimes \mathbb{E} + \mathbb{E} \otimes \sigma_z)(a^\dagger e^{i\Delta t} + a e^{-i\Delta t})$. When we choose the microwave pulse $\omega_{d3} = 4.5$ GHz, and $\omega_{d4} = 9.5$ GHz, respectively. The cross talk of the two coupling channels on CPB2, kinetic and exchange coupling, can be eliminated via rotating-wave approximation because of the chosen parameters $\Delta \gg \Delta_1$. Meanwhile, the driven of CPB 1 by ω_{d4} is neglecting small while $\delta_2 = \omega_{d4} - \omega_{r1} \gg \Delta$. Then, in the interaction picture, the complete Hamiltonian is

$$H = \frac{\hbar g}{2}(\sigma_z \otimes \mathbb{E} + \mathbb{E} \otimes \sigma_z)(a^\dagger e^{i\Delta t} + a e^{-i\Delta t}) + \frac{\hbar g}{2} i(a^\dagger - a)(\mathbb{E} \otimes \sigma_x). \tag{18}$$

Rotating on the CPB1 and CPB2, Hamiltonian (18) can be rotated to

$$H = \frac{\hbar g}{2}(\sigma_x \otimes \mathbb{E} + \mathbb{E} \otimes \sigma_y)(a^\dagger e^{i\Delta t} + a e^{-i\Delta t}) + \frac{\hbar g}{2} i(a^\dagger - a)(\mathbb{E} \otimes \sigma_x), \tag{19}$$

the effective Hamiltonian of which recover the 1D ME Hamiltonian in Eq. (4) with the identification of

$$p_x = i\sqrt{\frac{m'\hbar\omega_{r2}}{2}}(a^\dagger - a), \quad c = g\sqrt{\frac{\hbar}{2m'w_{r2}}}, \quad mc^2 = \frac{\hbar g^2}{2\Delta}, \tag{20}$$

where m' is the mass of inductance.

As mentioned above, to verify our simulation, we need to measure the Pseudo-helicity, which is conserved in ME. In Fig. 2, we numerically calculated the expectation value of *pseudo-hlicity* $\Sigma = \sigma_x p_x$ in both Dirac equation and ME. Obviously, the expectation value oscillate versus time in $1+1$ Dirac equation (the red line) but not in $1+1$ ME (the blue line). In our simulation, the initially spinor state is chosen as $\psi_{(k,t=0)} = \frac{\alpha^{1/2}}{(2\pi)^{1/4}} e^{-(\alpha k)^2} \begin{pmatrix} 1 \\ 1 \end{pmatrix}$, where $\alpha = \sqrt{\frac{\hbar}{2m'\omega_{r2}}} = 0.16 \times 10^{-16}$ with $m' = 3.3127 \times 10^{-12}$ and $\omega_{r2} = 10$ GHz, and the FWHM in k space is $\Delta k = \frac{1}{2\alpha}$. For convenience of comparison, we set the the third and fourth component of the spinor state initially to be zero in ME.

We now move to measure the Pseudo-helicity in circuit QED. We first deal with the kinetic part, which can be measured as following: 1) a state-dependent operator $U_2 = \exp(-ik(\mathbb{E} \otimes \sigma_y) \otimes p_x/2)$ acting on CPB 2, which can be generated by two microwave pulses with initial phases being π; 2) a σ_z measurement of CPB 2, which can be measured by microwave irradiation of the cavity and then probing the transition frequency if the qubit state is in excited state or not [9, 17]. The above two steps equal to the measurement of [11]

$$F(k) = U_2^{\dagger}(\mathbb{E} \otimes \sigma_z)U_2 = \cos(kp_x)(\mathbb{E} \otimes \sigma_z) - \sin(kp_x)(\mathbb{E} \otimes \sigma_x), \tag{21}$$

where k is determined by the probing time [9]. As $\frac{d}{dk}\langle F(k)\rangle\big|_{k=0} = -\langle(\mathbb{E} \otimes \sigma_x) \otimes p_x\rangle$, the kinetic term of Eq. (10) can be measured by probing the initial slope of the observable $F(k)$ [9]. Similarly, the second spin exchange interaction term in Eq. (10), can be measured by a unitary transformation $U_1 = \exp(-ik(\sigma_x \otimes \mathbb{E}) \otimes p_x/2)$ on CPB 1, and measure the spin correlation $\sigma_z \otimes \sigma_x$, for the former operation, an additional $\pi/2$ pulse is needed. Then probing the initial slope as before, we obtain $\frac{d\langle\sigma_z \otimes \sigma_x\rangle}{dk}\Big|_{k=0} = 2\langle(\sigma_y \otimes \sigma_x) \otimes p_x\rangle$. Combining both the kinetic and spin exchange terms, we achieve our final goal of measuring the Pseudo-helicity in Eq. (5).

Although the absolute value of Pseudo-helicity is small, it should not hamper our measurement since what we directly need to measure is σ_z. In circuit QED, high-fidelity quantum non-demolition measurements of σ_z is now an experimental routine [17]. In the follwing, we highlight the measurement process in our scheme with input-output process. In our model, if the cavity contains two qubits, the intracavity field come from b_{in} will acquire some nontrivial dynamics which then compel the external field a_{out} to have a time dependence different from the free field dynamics (cf. Fig. 3). Then there is a qubit-state-dependent phase shift between the input and output fields [20].

As we all know that there is an associated loss mechanism in all physical process, particularly in measurement scheme, the loss strongly influence the precise quantum non-demolition measurement, such as regulating and controlling, so the dispersive regime should be considered in measurement mechanics. In-

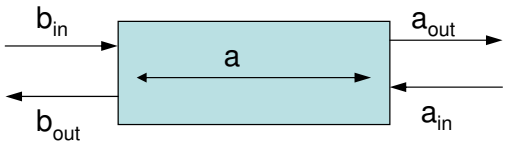

FIG. 3: A schematic representation of the cavity field, input field and output field for a two-side leady cavity

sight into the dispersive regime between the CPB 1 and the intracavity can be obtained by the unitary transformation

$$U_1 = \exp\left[\frac{g}{\Delta'}(a\sigma_+ - a^\dagger\sigma_-)\right], \tag{22}$$

where large detuning $\Delta' = \omega_{r1} - \omega_1 \gg g$. Applying transformation (22) to the Hamiltonian (8) and (9) to second order in g (neglecting the damping for the moment), for CPB 1, we can get

$$\begin{aligned} H_{sys1} &= U_1(H_{JC} + H_d)U_1^\dagger \\ &\approx \hbar(\omega_{r1} - \omega_{d3})a^\dagger a + \frac{\hbar}{2}(\omega_1 - \omega_{d3})\sigma_z + \frac{\hbar g^2}{\Delta'}a^\dagger a\sigma_z + \frac{\hbar g^2}{2\Delta'}\sigma_z + \frac{\hbar g\varepsilon}{\Delta'}\sigma_x + \hbar\varepsilon(a^\dagger + a) \end{aligned} \tag{23}$$

in a rotating frame at the drive frequency ω_{d3}.

We can consider the resonator as a two-side leaky cavity with equal rates, as shown in Fig. 3. The relationship between the input and the output mode can be written as $a_{out}(t) = \sqrt{\kappa}a(t) - a_{in}(t)$, where a_{out} and a_{in} is the output mode and input mode at the output port respectively, a is the intracavity mode, and cavity lifetime $1/\kappa$ is about $160ns$ in a typical circuit QED system [15]. The quantum voltage is related to the current carried by the TLR by $I(x,t) = \sqrt{\frac{c}{l}}V(x,t)$. For the moment, it is more convenient to have stationary rather than traveling quantum voltage. For this mode, we have following equation of motion for the CPB 1

$$\begin{aligned} \frac{da(t)}{dt} &= -\frac{i}{\hbar}[a(t), H_{sys1}] - \kappa a(t) + \sqrt{\kappa}a_{in}(t) + \sqrt{\kappa}b_{in}(t) \\ &= -i[(\omega_{r1} - \omega_{d3})a + \varepsilon + \chi_1 a\sigma_z] - \kappa a(t) + \sqrt{\kappa}a_{in}(t) + \sqrt{\kappa}b_{in}(t), \end{aligned} \tag{24}$$

where $\chi_1 = g^2/\Delta'$ and b_{in} is the input mode at the input port of the resonator. Applying Fourier transformation on the above expression and rearranging, we can obtain a spectra function between the input and the output mode

$$a_{out}(\omega) = \frac{\kappa\left[a_{in}(\omega) + b_{in}(\omega)\right] - i2\pi\sqrt{\kappa}\varepsilon\delta(\omega)}{\kappa + i(\chi_1\sigma_z + \omega_{r1} - \omega_{d3} - \omega)} - a_{in}(w) \tag{25}$$

where $\delta(\omega)$ is the Dirac function. Obviously, the σ_z in the denominator is a formal indication that the output spectra depend on the qubit state ($\sigma_z = \pm 1$). In the case $\omega = \omega_{r1} - \omega_{d3}$, we can get [21]

$$a_{out}^{\mp}(w_{r1} - \omega_{d3}) = \frac{\kappa b_{in}(\omega_{r1} - \omega_{d3})}{\kappa \pm i\chi_1} \mp \frac{i\chi_1}{\kappa \pm \chi_1} a_{in}(\omega_{r1} - \omega_{d3}). \tag{26}$$

We can assume that $a_{in}(t)$ is always the vacuum because of the very small reflection and backscatter of the resonator. Furthermore, the two input modes are assumed to be independent and we have neglected the two-photo process. Therefore, $a_{in}(w)$ has no contribution to the normally ordered moment $a_{out}(w)$, and thus

$$\langle a_{out}^{\mp}(\omega_{r1} - \omega_{d3})\rangle_{\mathcal{N}1} = \left\langle \frac{\kappa b_{in}(\omega_{r1} - \omega_{d3})}{\kappa \pm i\chi_1} \right\rangle_{\mathcal{N}1} = \langle e^{i\theta_1^{\pm}} \tilde{b}_{in}(\omega_{r1} - \omega_{d3})\rangle_{\mathcal{N}1}, \tag{27}$$

where $\langle\cdot\rangle_{\mathcal{N}}$ signify a normally ordered moment, $\theta_1^{\pm}$ is the phase shift dependent on the qubit state between the input field b_{in} and the output field a_{out} [$\tan(\theta_1^{\pm}) = \mp\frac{g^2}{\Delta'\kappa}$] and $\tilde{b}_{in}$ is a scaled quantity of b_{in}. When the cavity resonance frequency and drive frequency is confirmed, the phase shift dependent on the CPB1 qubit state is about $\pm\frac{134\pi}{360}$ and the corresponding frequency interval is 29.6 MHz for our scheme, which is readily resolvable experimentally [15].

Similarly, analogical transformation can be applied on CPB 2, we can obtain

$$\langle a_{out}^{\mp}(\omega')\rangle_{\mathcal{N}2} = \left\langle \frac{\kappa b_{in}(\omega')}{\kappa \pm i\chi_2} \right\rangle_{\mathcal{N}2} = \langle e^{i\theta_2} \tilde{b}_{in}(\omega')\rangle_{\mathcal{N}2}, \tag{28}$$

where $\omega' = \omega_{d1} + \omega_{d2} + \omega_{d4} - \omega_{r2}$, $\tan(\theta_2^{\pm}) = \frac{\mp g^2}{\Delta''\kappa}$ and $\chi_2 = g^2/\Delta''$ with $\Delta'' = \omega_{r2} - \omega_2 \gg g$. For the CPB2, $\theta_2 = \pm\frac{268\pi}{360}$ and the frequency interval is 59.2 MHz.

In summary, we propose to simulate ME with two CPB capacitively coupled to the TLR in circuit QED system where we are able to engineer different kinds of interaction which constructing the wanted Hamiltonian for ME. The conserved observable pseudo-helicity is measured via the input-output process, estimation based on conservative parameters shows that it is experimentally resolvable.

This work was supported by National Fundamental Research Program of China (Grant No. 2013CB921804, No. 2011CB922104 and No. 2011CBA00200), National Natural Science Foundation of China (Grant No. 11004065, No. 60978009, and No. 91121023), the Program for Changjiang Scholars and Innovative Research Team in University, the project of Educational Commission of Hubei Province (No. Q20112501 and No. 2010C20).

[1] J. I. Cirac and P. Zoller, Nature Phys. **8**, 264 (2012).

[2] B. Thaller, *The Dirac equation* (Springer-Verlag, Berlin, 1992).

[3] C. L. Kane and E. J. Mele, Phys. Rev. Lett. **95**, 226801 (2005).

[4] S.-L. Zhu, B. Wang, and L.-M. Duan, Phys. Rev. Lett. **98**, 260402 (2007).

[5] G. Juzeliūnas, J. Ruseckas, and M. Lindberg, L. Santos, and P. Öhberg, Phys. Rev. A **77**, 011802 (2008).

[6] J. Ruseckas, G. Juzeliūnas, P. Öhberg, and M. Fleischhauer, Phys. Rev. Lett. **95**, 010404 (2005).

[7] S.-L. Zhu, H. Fu, C.-J. Wu, S.-C. Zhang, and L.-M. Duan, Phys. Rev. Lett. **97**, 240401 (2006).

[8] L. Lamata, J. León, T. Schätz, and E. Solano, Phys. Rev. Lett. **98**, 253005 (2007); J. Casanova, J. J. García-Ripoll, R. Gerritsma, C. F. Roos, and E. Solano, Phys. Rev. A **82**, 020101 (2010).

[9] R. Gerritsma, G. Kirchmair, F. Zähringer, E. Solano, R. Blatt, and C. F. Roos, Nature **463**, 68 (2010).

[10] F. Wilczek, Nature Phys. **5**, 614 (2009).

[11] J. Casanova, C. Sabín, J. León, I. L. Egusquiza, R. Gerritsma, C. F. Roos, J. J. García-Ripoll, and E. Solano, Phys. Rev. X **1**, 021018 (2011).

[12] J. Q. You and F. Nori, Nature **474**, 589 (2011); Phys. Today **58**(11), 42 (2005).

[13] Y. Makhlin, G. Schön, and A. Shnirman, Rev. Mod. phys. **73**, 357 (2001).

[14] A. A. Houck, H. E. Türeci, and J. Koch, Nature Phys. **8**, 292 (2012).

[15] A. Wallraff, D. I. Schuster, A. Blais, L. Frunzio, R.- S. Huang, J. Majer, S. Kumar, S. M. Girvin, and R. Schoelkopf, Nature **431**, 162 (2004).

[16] S.-L. Zhu, C. Monroe, and L.-M. Duan, Phys. Rev. Lett. **97**, 050505 (2006).

[17] A. Blais, R.-S. Huang, A. Wallraff, S. M. Girvin, and R. J. Schoelkopf, Phys. Rev. A **69**, 062320 (2004).

[18] Z.-Y. Xue, Quantum Inf. Process. **11**, 1381 (2012).

[19] E. Solano, G. S. Agarwal, and H. Walther, Phys. Rev. Lett. **90**, 027903 (2003).

[20] D. F. Walls, G. J. Milburn, *Quantum Optics* (Springer-Verlag, Berlin, 2008), chap. 7.

[21] M. Sarovar, H.-S. Goan, T. P. Spiller, and G. J. Milburn, Phys. Rev. A **72**, 062327 (2005).

[22] A. Zee, *Quantum field Therory in a Nutshell* (Princeton University Press, Princeton, 2003).